Journal of Polymer Research (2019) 26: 62
https://doi.org/10.1007/s10965-019-1724-6

ORIGINAL PAPER

Design and fabrication of environmentally benign cellulose based hydrogel matrix for selective adsorption of toxic dyes from industrial effluvia

Kabiru Bello [1] · Balladka Kunhanna Sarojini [1] · Badiadka Narayana [2]

Received: 3 September 2018 / Accepted: 1 February 2019 / Published online: 12 February 2019

Abstract

The present study investigates the use of agri-waste derived superabsorbent graft copolymer for effective removal of hazardous dye from industrial effluents. The hydrogel was synthesized via free radical graft copolymerization of poly (3-acrylamidopropyl)-trimethylammonium chloride copolymer N,N-Dimethylacrylamide (APTAC-co-DMA) onto banana pseudo-stem carboxymethyl cellulose (BPCMC) backbone. The reaction was initiated by ammonium per sulfate (APS) whereas the polymer cross linking was achieved by the addition of N,N-methylene-bis-acrylamide (MBA). The hydrogel was evaluated for its structure, morphology and thermal behavior using FT-IR, FESEM and TGA analyses respectively. The parameters affecting the hydrogel's swelling capacity in distilled water were optimized and the optimum condition was used to perform pH sensitivity test on the hydrogel. The maximum swelling as high as 559 g/g was obtained at the optimized condition of 0.0657 mol/L, 0.0972 mol/L and 0.5 mol for APS, MBA and APATAC/DMA respectively. The pH sensitivity test revealed maximum swelling under pH 7 for 570 min. Furthermore, the hydrogel was evaluated for removal of Rhodamine B. (RhB) and Eriochrome black T (EBT) dyes. The respective maximum dye adsorption capacity to the tune of 434 and 714 mg/g for RhB and EBT was obtained. The adsorption was modeled for isotherm studies and the Freundlich isotherm model was found to be the most favored models befitting the adsorption of both dyes.

Keywords Agri-waste · (3-acrylamidopropyl)-trimethylammonium chloride · N,N-Dimethylacrylamide · Rhodamine B. · Eriochrome black T

Introduction

Undoubtedly, water is an indispensable commodities not only for human survival, but for perpetual prosperity of both developed and developing nations [1]. Albeit 75% of earth is covered by water, only about 2.5 percent of world's total water content is fresh, water of which just about 1% is accessible for domestic, agricultural and industrial usage [2]. This limited amount of world's fresh water is stagnant and the world's population is drastically increasing resulting in enormous evolution of chemical industries. The evolution of various industries brings about the pollution of both surface and ground water reservoirs owing to the discharge of contaminants form municipals, agricultural and industrial sources [2]. In addition to the heavy metal contamination by the chemical industries, the alarming quantity of dye containing effluvia from various chemical industries like textile industries poses serious esthetic and toxicological threat to water bodies [3].

The annual consumption and production of dye by the chemical industries particularly textile industry is reported to be to the tune of 7×10^5 [4]. A greater percentage of about 10–15% of the dye consumed by the textile industries ended of being discharge into the water bodies in the course of dyeing processes with 2×10^5 being oozed out as effluvia [5]. This constitutes inauspicious effects on aquatic lives and by extension, human health. The curious thing about the presence of dyes in water is its stability and tediousness in its removal conferred to it by aromatic structure it possesses. The aromatic

✉ Balladka Kunhanna Sarojini
bksaroj35@gmail.com

[1] Department of Industrial Chemistry, Mangalore University, Mangalagangothri, Karnataka State 574 199, India

[2] Department of Studies in Chemistry, Mangalore University, Mangalagangothri, Karnataka State 574 199, India

and azo group such as benzidines and naphthalenic derivatives present in dye structure are associated with toxic, mutagenic and sometimes carcinogenic implications in human. Moreover, the presence of minute quantity of azo dye unfavorably affects plant's photosynthetic activities thereby preventing the penetration of light and oxygen [5].

Rhodamine B. is a basic and cationic dye with a chemical formula $C_{28}H_{31}ClN_2O_3$. It is widely used in textile and paper industries as pigment and staining reagent for the determination of oils and fats. Rhodamine B. finds application in biotechnology and biology in fluorescence microscopy and in the determinations of rate flow and direction of water respectively. However, in spite of these favorable hallmarks, Rhodamine B. contains xanthenes and aromatic rings which are toxic, irritating to skin and cancer causing [6].

Eriochrome black T. is an azo dye that is used in complexometric titrations for determination of water hardness and for biological staining. It also used as colorant in textile and paper industries. However, the degradation product of Eriochrome black T. such as naphthaquinone is toxic and carcinogenic. These make the removal of Eriochrome black T. and Rhodamine B. dyes from waste water an issue of paramount importance [7].

Over the past decades, various physical, biological and chemical treatment methods for the removal of dyes from waste water were investigated. Methods such as membrane separation [8], chemical precipitations [9], coagulation/flocculation [10], oxidation [11] and electrochemical method [12] have been reported. These methods are proven effective in dye removal from waste water but are however associated with various constraints ranging from their low efficiency, difficulty in sludge disposition, selectivity in the type of dye to be removed, high operational cost and more importantly, the toxicity of their breakdown products [5].

Among various treatment methods mentioned above, adsorption may be regarded as the most favorable technique because of its high efficiency, cost effectiveness, user-friendliness and recyclability in comparison to the reported methods [13]. Extensive researches on the use of activated carbon as adsorbent for dye removal have been reported elsewhere [14]. Although being able to absorb appreciable quantity of dye from waste water, the use of activated carbon as adsorbent for dye removal suffers some shortcomings such as high energy involvement in the production and regeneration processes [15].

Until recently, researchers are paying attention to the use of nano materials such as nano crystals and nano composite as adsorbents for removal of different kinds of pollutants from waste water more than do the several conventional adsorbent in use today because of their high surface area, good mechanical strength and multi-functionality [16]. However, the use of nano materials in water treatment is associated with the uncertainty in their separation which entails high speed centrifugation and coagulation. The use of hydrogel as adsorbent for dye removal has been reported to be promising alternative to solving the aforementioned predicaments [17]. To cite a few, a good number of cationic as well as anionic superabsorbent hydrogels of carrageenan grafted polyacrylamide/bentonite cross linked with methylene bis-acrylamide [18], bis[2-(methacryloyloxy)ethyl] phosphate cross linked poly(acrylamide-co-AMPS) hydrogel [19], carrageenan grafted poly (acrylamide-co-sodium acrylate)/Montmorillonite composite hydrogel cross linked with methylene bis-acrylamide [20] and aliginate/PVA silver nanocomposite hydrogel [21] have been explored for dye adsorption.

Hydrogels are three-dimensional structured polymer networks that are able to absorb enormous amount of fluid more than hundred times their mass due to the presence of hydrophilic groups in their structure [22]. The intriguing aspect of these polymers is that, they are not only able to absorb high quantity of water but can conserve same and remain insoluble in the swelling medium. The hydrogels' water retention capacity is provided by the presence of crosslink in the polymer network. These hydrophilic groups which are often ionic create an elevated osmotic pressure difference between the polymer and the swelling medium which cause an inflow of large amount of water into the polymer networks [23]. This makes them preferred candidates for various applications in biomedicines [24], personal hygiene products [25], contact lenses [26], agriculture [27], cosmetics [28], water treatment [29], tissue engineering [30], slow release of fertilizers [31] and so forth.

Synthetic hydrogels are made from acrylic acid and its derivatives which are obtained from byproducts of petroleum. They are non-biodegradable, non-biocompatible and can be detrimental to the ecosystem [32]. Hydrogels prepared from natural sources such as karaya [33], gum gelatin [34], sodium aliginate [35], gum-gatti [36], chitosan [37], maize bran [38] and cellulose [39] have been reported. They are biodegradable, biocompatible and renewable in nature.

The most abundant natural polymer on earth is cellulose [40]. It is the major structural constituent in plant accounting for half to one-third component of plant tissue. It is proficient in the production of different industrial products ranging from paper products, biopolymers and biocomposites providing stability and mechanical strength [41]. Moreover, cellulose is biodegradable, renewable, abundant and biocompatible.

However, despite these favorable hallmarks, the industrial applications of cellulose are limited owing to its inability to dissolve in water and most organic solvents [42]. The insolubility of cellulose may be attributed to the stringent intra and inter molecular hydrogen bonding [15]. Despite several attempts to develop a solvent systems such as dimethyl sulfoxide/tetrabutylammonium fluoride, N,N-dimethylacetamide/lithium chloride and NaOH/urea to dissolve cellulose, concern about various environmental

constraints as well as difficulty in their recycle is at stake [43]. Cellulose is therefore transformed into its derivatives such as ethyl cellulose, cellulose acetate; carboxymethyl cellulose, etc. carboxymethyl cellulose is a water soluble substance which possesses cellulose properties with excellent pH sensitivity [43].

The exploration of diverse agricultural by-products such sugarcane bagasse [40], durian rind [43], wheat straw [32], Pomelo peel [44] and water hyacinth [45] to produce cellulose have been investigated. Utilizing agricultural waste to produce cellulose has great significance in minimization of biological waste and environmental pollution.

Banana pseudo-stem is a bye product from banana plant which is among the popular fruit cultivated not only in India but in Thailand, Malaysia and Thailand with higher production in India to the tune of 14.2 million tons per annum [46]. Despite being a promising and cheap source of cellulose, banana pseudo-stem is underutilized. We only know of few reports on the application of banana pseudo-stem fibers in paper, fertilizer and fiber making [47]. To the best of our knowledge, there is not a single report on the utilization of banana pseudo-stem for preparation of hydrogels if not for the previous work reported by our research group [48].

The present study reveals the preparation of hydrogel derived from banana pseudo-stem carboxymethyl cellulose via free radical graft copolymerization reaction. The grafting of poly (APTAC-co-DMA) on to banana pseudo-stem carboxymethyl cellulose was achieved using APS as initiator and the cross linking was made possible with help of MBA. The hydrogel was characterized by Fourier-transform infrared spectroscopy (FT-IR), field emission scanning electron microscopy (FESEM) and thermo gravimetric analysis (TGA). The pH sensitivity test on the prepared hydrogel was conducted by swelling the hydrogel in solutions of varied pH. Furthermore, the ability of the prepared hydrogel to adsorb Rhodamine B. and Eriochrome black T. was studied and the adsorption kinetics and isotherm models were explored.

Experimental

Materials

The carboxymethyl cellulose used in this study was prepared in our laboratory using a reported method [44]. The distilled water used in this experiment was prepared in our laboratory. Ethanol (95%) and toluene (99%) as solvents for cellulose extraction from banana pseudo-stem fibers were purchased from Spectrochem Mumbai, India. Sodium hydroxide (98%), sodium hypochlorite (6%), Eriochrome black T. and Rhodamine B. were provided by Loba Chemie Lab. Reagents and Fine chemicals Mumbai, India. Isopropyl alcohol (99%), sodium monochloroacetate (98%), ammonium per sulfate (98%) and N,N-methylene-bis-acrylamide (99%) were procured from Himedia Mumbai, India. 3-(Acrylamidopropyl)-trimethylammonium chloride (75 wt% in water) and N,N-Dimethylacrylamide (99%) used as monomers for free radical graft copolymerization were purchased from Sigma Aldrich chemicals Mumbai, India. All chemicals and solvents used in this experiment were of analytical grade and were used as received from their respective manufacturers without prior purification.

Synthesis of BPCMC grafted poly (APTAC-co-DMA) copolymer

BPCMC-g-poly (APTAC-co-DMA) hydrogel was prepared via free radical copolymerization of poly (APTAC-co-DMA) onto BPCMC using APS and MBA as initiator and cross linking agent respectively. Initially, a pre-measured quantity (0.5 g) of BPCMC was transferred into 100 mL beaker containing 20 mL distilled water and stirred for 10 h until a clear solution was observed. Afterwards, 0.0657 mol/L solutions of APS were added under continuous stirring at 50 ^{O} C for 15 min to generate free radicals. This was followed by the addition of varied amount of APTAC (0.5–2.5 mol) and DMA (0.5–2.5 mol) into the reaction mixture. After specified time interval, 0.0972 mol/L of MBA solution was added and the temperature was risen to 80 ^{O} C and the reaction continued for further 5 h under room condition. Subsequently, the gelled product obtained (hydrogel) was allowed to cool over night and then freed of homopolymer by transferring same in three-fold of acetone for 3 h. subsequently, the hydrogel obtained was rigorously washed with distilled water for removal of unreacted monomers [49]. The hydrogel was oven dried to a constant weight and kept in plastic pouch for future use. The grafting percentage and efficiency were evaluated using Eq. 1&2 respectively.

$$G.P. = \frac{W_2 - W_0}{W_0} X\ 100 \quad (1)$$

$$G.E. = \frac{W_2 - W_1}{W_1} X\ 100 \quad (2)$$

Where; W_O, W_1 and W_2 represent the weight of BPCMC, (APTAC + DMA) and BPCMC-g-poly (APTAC-co-DMA) after the homopolymer removal respectively.

Instrumental analysis

The structure of BPC extracted, BPCMC prepared and BPCMC-g-poly (APTAC-co-DMA) hydrogel prepared were confirmed by characterizing same with FT-IR spectrophotometer (Model: IR Prestige-21, Shimadzu Corporation, Japan). A pre-measured and triturated oven dried samples were mixed with a known quantity of KBr to form pellets and the samples

were evaluated for their functional group using attenuated transmission method. The spectra of the analyzed samples were recorded from 400 to 4000 cm^{-1} frequency range.

Surface morphology of BPC extracted, BPCMC and BPCMC-g-poly (APTAC-co-DMA) prepared were observed by Field Emission Scanning Electron Micrograph (Carl Zeiss Microscopy Ltd). Prior to the analysis, the samples were gold coated using sputtering techniques for 15 min and the micrograms were observed and magnified using 15 kv accelerating voltage.

The thermal stability of BPC extracted, BPCMC and BPCMC-g-poly (APTAC-co-DMA) hydrogel prepared were analyzed using thermo gravimetric analyzer (Model; SDTQ600, TA Instruments, UK). Briefly, a pre-measured quantity (5–7 mg) of the analytes were introduced into the thermo gravimetric analyzer under nitrogen atmosphere with a gas flow rate of 100 mL/min. The samples were heated at the rate of 10 °C/min in a temperature range of 25–700 °C.

Determination of water uptake capacity of hydrogel

The prepared BPCMC-g-poly (APTAC-co-DMA) hydrogel was evaluated for its swelling ability in distilled. Initially, the hydrogel was cut into small pieces and the pre-measured (100 mg) amount of hydrogel was immersed in a 100 mL beaker containing 50 mL distilled water. The suspension containing the prepared hydrogel was placed on a magnet stirrer at a stirring speed of 120 rpm for 570 min for attainment of equilibrium swelling. After a preset interval of time (0–570 min), the swollen BPCMC-g-poly (APTAC-co-DMA) hydrogel was withdrawn from the swelling medium, drained of the surface water with the aid of filter paper and weighted. The swelling equilibrium in g/g was evaluated using Eq. 3.

$$Q_{eq} = \frac{M_2 - M_1}{M_1} \tag{3}$$

Where; Q_{eq}, M_1 and M_2 are the equilibrium swelling, weight of dry and swollen BPCMC-g-poly (APTAC-co-DMA) respectively.

Effect of pH and contact time on swelling capacity of BPCMC-g-poly (APTAC-co-DMA) hydrogel

The effect of pH and contact time on swelling capacity of the prepared BPCMC-g-poly (APTAC-co-DMA) hydrogel was investigated. In a typical experiment, a known quantity (100 mg) of the prepared BPCMC-g-poly (APTAC-co-DMA) hydrogel was immersed into a beaker containing 100 mL of test solution of known pH. This was sequel to the preparation of solutions of varied pH (1–13) by transferring the required buffer capsule equaling the targeted pH in 100 mL distilled water. The maximum swelling of BPCMC-g-poly (APTAC-co-DMA) hydrogel in each of pH solutions prepared was calculated from Eq. 4. Furthermore, the effect of contact time against the swelling capacity of the prepared BPCMC-g-poly (APTAC-co-DMA) hydrogel was determined using the pH solution in which the hydrogel exhibited maximum swelling capacity under a preset time interval of 0–570 min. at each time interval, the swollen hydrogel is withdrawn from the beaker containing the test solution, filtered off the surface water and re-weighted [47]. Equally, the swelling equilibrium was evaluated using Eq. 3.

Preparations of dye solution

The preparation of Rhodamine B. and Eriochrome black T. dyes used in this experiment followed a reported method by [50]. Briefly, a pre-measured (100 mg) quantity of dye powder was placed into 250 mL conical flask containing 100 mL of distilled water. The solution was mechanically swirled for complete dissolution of dye [50] afterwards; the solutions of varied concentration were prepared from the 1000 mg/L dye solution using dilution formula.

Dye uptake studies

The adsorption of Rhodamine B. and Eriochrome black T dyes on the prepared BPCMC-g-poly (APTAC-co-DMA) hydrogel was performed via batch adsorption technique. This was carried out by immersing a pre-measured amount of the prepared BPCMC-g-poly (APTAC-co-DMA) hydrogel in to a beaker containing 500 mL solution of known dye concentration. The beaker was covered with aluminum foil paper and placed on magnetic stirrer under constant stirring speed of 120 rpm for a designated time interval of 0–570 min. at each preset interval of time, 5 mL of dye solution was withdrawn from the test solution, then centrifuged for 2 min to remove suspended polymer and analyzed with UV-Vis spectrometer (UV-1800, Shimadzu Corporation, Japan). The UV-Vis spectra of each of the analyte was recorded in the wavelength range of 200–800 nm and the concentration of each sample was evaluated from the absorption at λ_{max} using linear regression curve obtained from calibration curve over concentration range [51]. The dye uptake capacity of the hydrogel was calculated using Eq. 4.

$$q_e = \frac{(C_0 - C_e)}{M} X V \tag{4}$$

Where; q_e (mg/g) is the adsorption capacity at equilibrium, C_o and C_e represent the initial and equilibrium concentration of dye (mg/L) in solution respectively, M (mg) is the weight of the adsorbent and V (ml) is the volume of dye solution used.

Dye adsorption and re-use experiment

Dye adsorption and re-use experiments were conducted so as to ascertain the reusability of the adsorbent over different cycles. Typically, 50 mg of the prepared hydrogel was kept in contact with 50 mL of aqueous dye solution whose concentration was maintained at 50 mg L^{-1} for a specified period of time to allow for maximum adsorption of dye. Following the attainment of equilibrium, the hydrogel was removed from the adsorption medium and utilized for re-use process. The desorption process was performed by immersing a dye loaded hydrogel in 50 mL of distilled water as desorption medium with certain pH adjusted by NaOH or HCl solution at room temperature. The solutions were stirred on a magnetic stirrer for a period of 30 min until reaching equilibrium at room temperature. The hydrogel was removed from the solution, washed severally with distilled water to get rid of the surface dye and finally dried in hot air oven at 50 °C for subsequent cycles and the amount of dye desorbed in the aqueous solution was determined by UV–VIS spectrophotometer. The re-use processes were conducted for three consecutive cycles and the desorption efficiency (D %) was calculated using Eq. 5.

$$D\,(\%) = \frac{C_d V_d}{(C_o - C_e)V_i} \quad X\ 100 \tag{5}$$

Where C_0 and C_e are the initial and the equilibrium concentration of the dye solution whereas C_d is the concentration of the dye in the desorption solution. V_i and V_d are the volume of the adsorption solution and the desorption solution (mL) respectively.

Results and discussion

Mechanism of preparation of BPCMC-g-poly (APTAC-co-DMA) hydrogel

The BPCMC prepared in our laboratory was used to synthesize BPCMC-g-poly (APTAC-co-DMA) hydrogel via free radical graft copolymerization reaction of APTAC and DMA onto BPCMC backbone. The reaction uses APS and MBA as initiator and cross linking agent respectively. The proposed mechanism is as shown in Scheme 1. Initially, the mild temperature (50 °C) treatment of APS initiator resulted in the formation of sulfate anion-radical which reacted with BPCMC leading to the abstraction of hydrogen from the hydroxyl group of BPCMC chains to form BPCMC macro radical. The BPCMC macro radical generated reacted with active vinyl group of APTAC and DMA which are in close proximity with BPCMC macro radical leading to the chains propagation step. At this stage, the terminal vinyl group of MBA cross linker reacted with the polymer chains to produce a cross linked structured network. Finally, the combination of radicals brings about the growth termination of graft copolymer.

Optimization of graft copolymerization parameters on swelling capacity of BPCMC-g-poly (APATAC-co-DMA) hydrogel

Effect of varied parameters affecting the swelling capacity of the prepared BPCMC-g-poly (APTAC-co-DMA) hydrogel was investigated and the result is depicted in Table 1. The optimized condition for BPCMC, APS and MBA concentration was found to be 0.5 g, 0.0657 mol/L and 0.0972 mol/L respectively. Only the effect monomer ratio on swelling capacity of the prepared hydrogel was investigated in this study. The optimum concentrations of APS, BPCMC and MBA were used as reported in the previous study published by our research group [48]. In a typical experiment, varied concentrations (0.5–2.5 mol) of APTAC/DMA were used to prepare different BPCMC-g-poly (APTAC-co-DMA) hydrogel and the hydrogels were labeled K_1-K_9 as presented in Table 1. The swelling capacity of each hydrogel prepared (K_1-K_9) was determined by swelling same in distilled water for a preset time interval. Initially, it was observed that, the swelling capacity of the hydrogels prepared increases with increase in the concentration of APATAC and DMA. The swelling capacity of the prepared hydrogels began to decline when the concentration of APTAC goes beyond 1.5 mol. The sharp decrease in swelling capacity of the prepared hydrogel when the monomers concentration increased could partly be attributed to the higher viscosity of the reaction medium on one hand and the preference of homopolymerization to graft copolymerization on the other hand. The increased viscosity of the reaction medium hinders the mobility of free radicals and monomer molecules thereby lowering their chances of partaking in the reaction. The maximum swelling (559.37 g/g) was obtained at the optimum concentrations of 1.5 mol and 0.5 mol for APTAC and DMA respectively.

Fourier-transform infrared spectroscopy (FT-IR)

The structure of BPC extracted, BPCMC and BPCMC-g-poly (APTAC-co-DMA) hydrogel synthesized was identified by Fourier-transform infrared spectroscopy using attenuated transmission method and the spectra were transcribed between 4000 and 400 cm^{-1} frequency ranges. The FT-IR spectrum of BPC exhibits the characteristics bands at 3320, 2925 and 1095 cm^{-1} which are assigned to –OH stretching vibration, -C-H stretching vibration and C-O stretching vibration respectively (Fig. 1a). These peaks are characteristics of functional group of cellulose as reported by [36]. Similarly; the FT-IR spectrum of BPCMC (Fig. 1b) prepared displays the characteristics peaks at 1650 cm^{-1} corresponding to stretching vibration of carbonyl group absorption. This is in addition to the

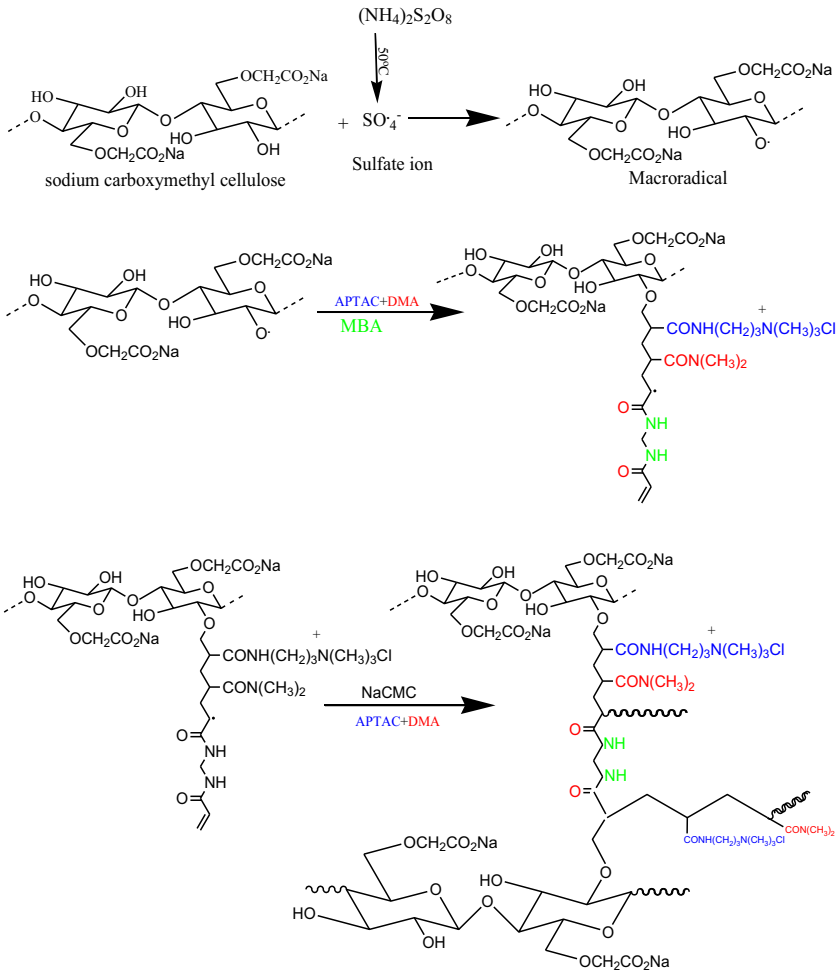

Scheme 1 Proposed reaction mechanism of APS initiated graft copolymerization of poly (APTAC-co-DMA) on BPCMC

characteristic peaks at 3320, 2925 and 1093 cm^{-1} which are ascribed to the –OH -C-H and C-O stretching vibrations respectively. This was taken as evidence to establish the successful etherification of BPC to form BPCMC [15]. However, as illustrated in Fig. 1c, the FT-IR spectrum of the prepared BPCMC-g-poly (APTAC-co-DMA) hydrogel displays the characteristic bands at 3390.52, 2924.38, 2853 and 1753 cm^{-1} which can be attributed to –OH stretching vibration, -CH_3 symmetric stretching vibration and C=O stretching vibration respectively. The characteristic peaks at 1613.08 and 1255 cm^{-1} can be assigned to secondary amide N-H stretching vibration and –C-N stretching vibration respectively [49]. Additionally, the characteristic bands at 1485 and 951.09 cm^{-1} are due to bending and stretching vibration of quaternary ammonium group respectively. Finally, the characteristic bands at 1101 and 874 cm^{-1} correspond to –

Table 1 Detailed feed compositions of the synthesized BPCMC-g-poly (APTAC-co-DMA)

Sample code	APTAC/DMA ratio	APTAC (mol)	DMA (mol)	MBA (mol/L)	APS (mol/L)	Swelling ratio (g/g)
K_1	1:1	0.5	0.5	0.0972	0.0657	480
K_2	1:2	0.5	1	0.0972	0.0657	134.34
K_3	1:3	0.5	1.5	0.0972	0.0657	131.15
K_4	1:4	0.5	2	0.0972	0.0657	115.00
K_5	1:5	0.5	2.5	0.0972	0.0657	113.50
K_6	2:1	1	0.5	0.0972	0.0657	159.33
K_7	3:1	1.5	0.5	0.0972	0.0657	559.37
K_8	4:1	2	0.5	0.0972	0.0657	548.29
K_9	5:1	2.5	0.5	0.0972	0.0657	336.92

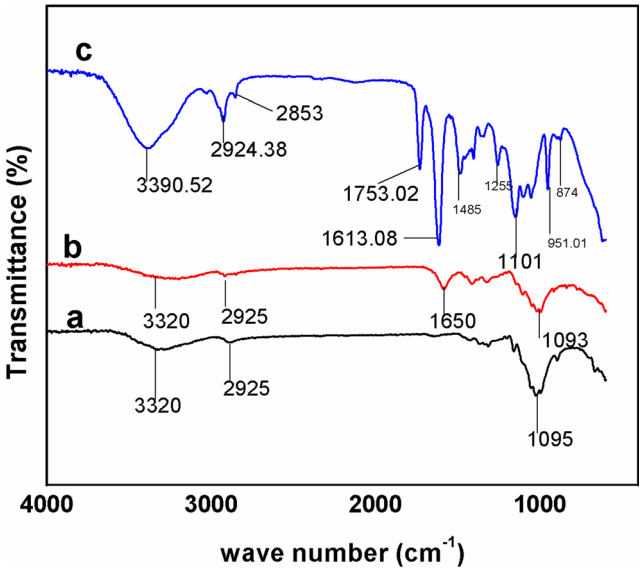

Fig. 1 FT-IR spectra of (**a**) BPC, (**b**) BPCMC and (**c**) BPCMC grafted poly APTAC-co-DMA

C-O and D-glucosidic bond stretching vibration respectively [52]. It is concluded thus; the observed difference between the FT-IR spectrum of BPC, BPCMC and BPCMC-g-poly (APTAC-co-DMA) hydrogel confirms the grafting of APTAC and DMA on to BPCMC.

Field emission scanning electron microscopy analysis

In order to investigate the shape and morphology of BPC extracted, BPCMC and BPCMC-g-poly (APTAC-co-DMA) hydrogel prepared, field emission scanning electron microscopy (FESEM) was accomplished and the micrographs are delineated in Fig. 2. As illustrated in Fig. 2a, the micrograph of BPC displays a more fiber-like structure which can be ascribed to the uncompromising self interaction of BPC chains occasioned by the inter and intra molecular hydrogen bonding [37]. The BPCMC micrograph portrays a rod-like structure (Fig. 2b) which may be accounted to etherification on OH groups of BPC chains. Conversely, the micrograph of the prepared BPCMC and BPCMC-g-poly (APTAC-co-DMA) hydrogel exhibited a coarser and porous surface of different size distribution. The porous and coarser surface portrayed by the prepared BPCMC and BPCMC-g-poly (APTAC-co-DMA) hydrogel might be responsible for entrapment of water molecules into the polymer network leading to the amplified dye adsorption capacity of the hydrogel and was used as

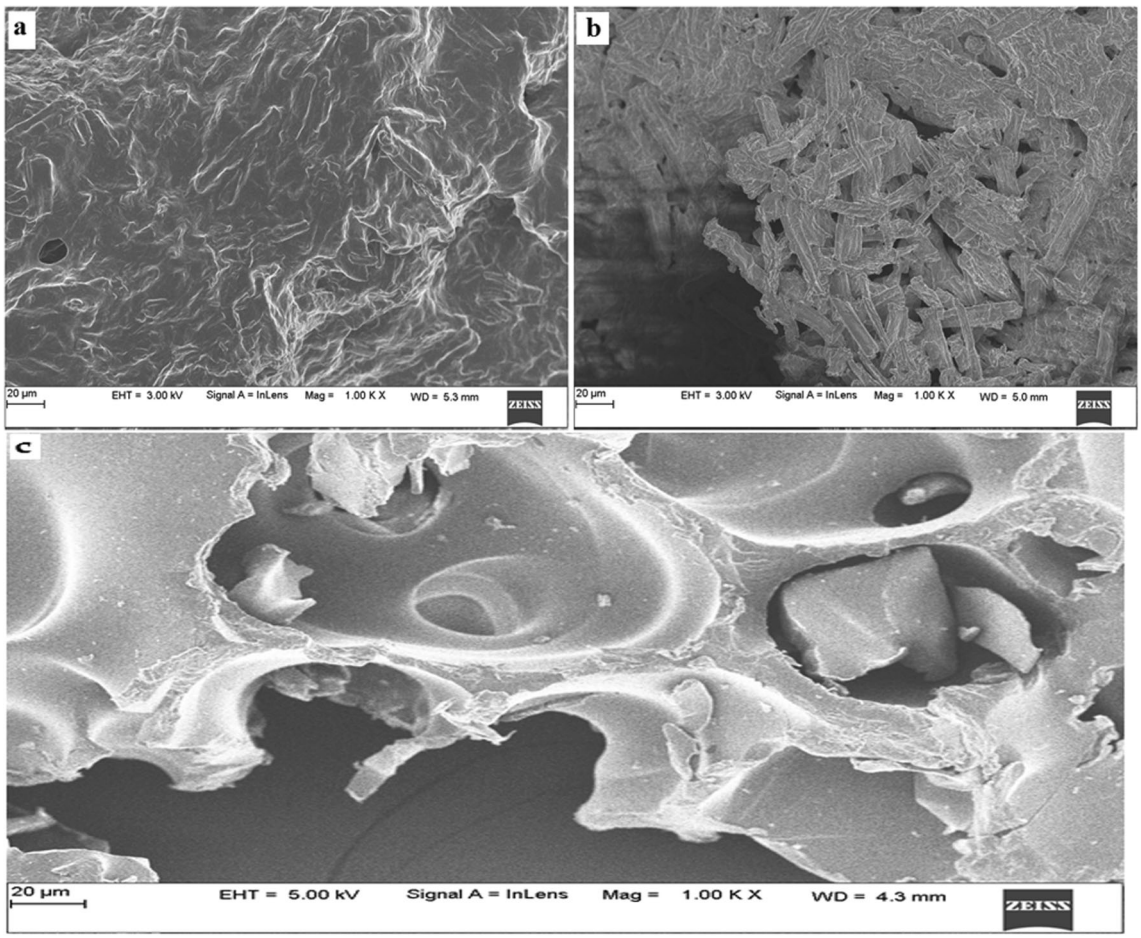

Fig. 2 FESEM images of (**a**) BPC, (**b**) BPCMC and (**c**) BPCMC-g-poly (APTAC-co-DMA)

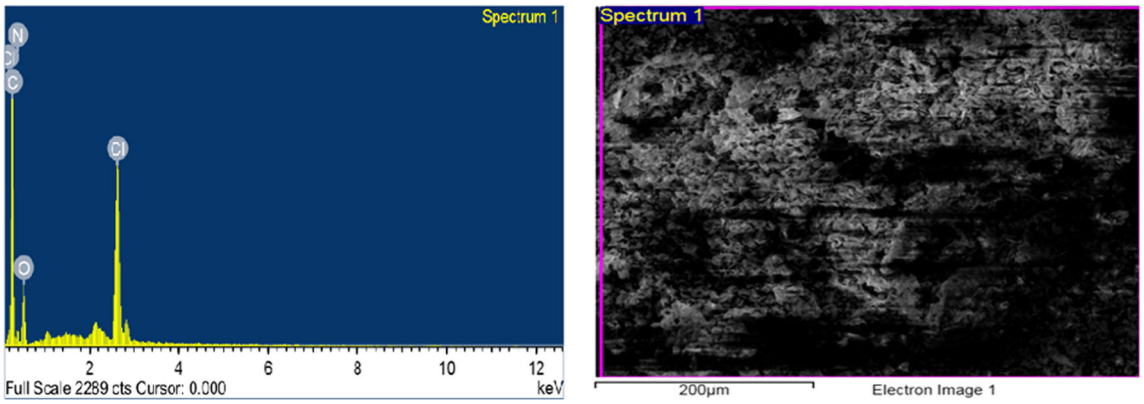

Fig. 3 EDS and Live image of BPCMC-g-poly (APTAC-co-DMA) graft copolymer

further evidence to affirm the successful grafting of APTAC and DMA onto BPCMC [53].

Energy dispersive X-ray spectroscopy

To further confirm the grafting of APTAC and DMA onto BPCMC backbone, the prepared BPCMC-g-poly (APATAC-co-DMA) hydrogel was subjected to Energy dispersive X-ray spectroscopic analysis so as to identify the elemental composition of the prepared hydrogel and the result is depicted in Fig. 3. The energy requirement for emission was the basis on which the relative abundance of elements was set out. The elements were identified base on the specific character corresponding to the energy absorption as difference of K_{ev} energy level. The relative abundance of the element corresponds to the height of the peak in the spectrum [54]. As illustrated in Fig. 3, the prepared BPCMC-g-poly (APATAC-co-DMA) hydrogel contains the atomic percentage of carbon (24.48%), nitrogen (19.72%), oxygen (40.00%) and chlorine (16.21%).

Thermo gravimetric evaluation of BPCMC-g-poly (APTAC-co-DMA) hydrogel

The thermal stability/behavior of BPC extracted, BPCMC and BPCMC-g-poly (APTAC-co-DMA) hydrogel prepared was evaluated by conducting the thermo gravimetric analysis (TGA) and the thermo grams are presented in Fig. 4. The thermo gram of BPC revealed degradation stages at varied temperature which was accompanied by proportionate loss in mass. From Fig. 4a, it is palpable that the initial degradation stage of BPC occurred between the temperature ranges of 21–107 °C which brings about little weight loss of about 14%. This loss in mass can be explained by loss of moisture absorbed by the sample. The second decomposition stage observed between 260 and 337 °C temperature ranges which resulted in a significant loss in mass of about 74% can be attributed to the thermal break down of carboxyl and hydroxyl group containing compounds [55]. The third degradation stage observed between 310 and 700 °C temperature ranges which resulted in loss in weight of 96% leaves behind 4% residue as ash. Similar result was reported by [34]. Similarly, the thermo gram of BPCMC depicted in Fig. 4b revealed three degradation stages at 21–94 °C, 260–310 °C and 310–700 °C which resulted in loss in mass of 6 wt%, 28 wt% and 50 wt% respectively. The first and second degradation stages can be explained by loss in moisture content of the sample and thermal decomposition of carboxyl and hydroxyl groups in the cross linked polymer network respectively as reported by [38]. The thermo gram of the prepared BPCMC-g-poly (APTAC-co-DMA) hydrogel displayed three degradation stages as illustrated in Fig. 4c. The first degradation stage eventuated within the temperature range of 125–214 °C which resulted in a weight loss amounting to the 8 wt%. The weight loss of this sort is better explained by the loss in moisture content of the prepared BPCMC-g-poly (APTAC-co-DMA) hydrogel. The second degradation stage eventuated at 427–497 °C resulted in the major loss in mass of 76 wt%. The degradation stage can be attributed to the decomposition of carboxyl and hydroxyl group containing compounds. The

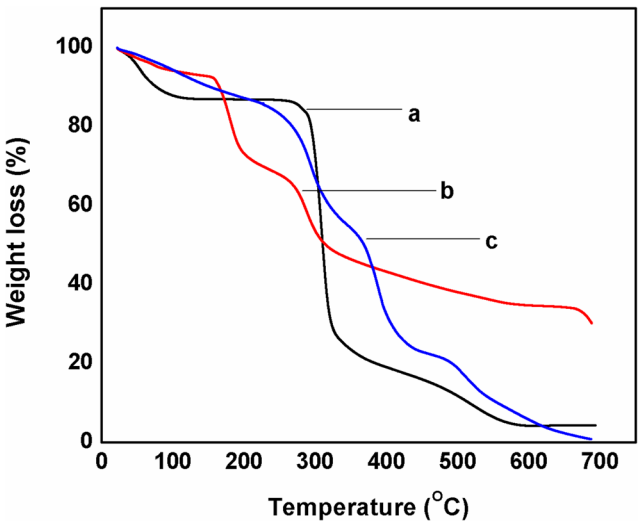

Fig. 4 TGA patterns of (**a**) BPC, (**b**) BPCMC and (**c**) BPCMC grafted poly (APTAC-co-DMA) hydrogel

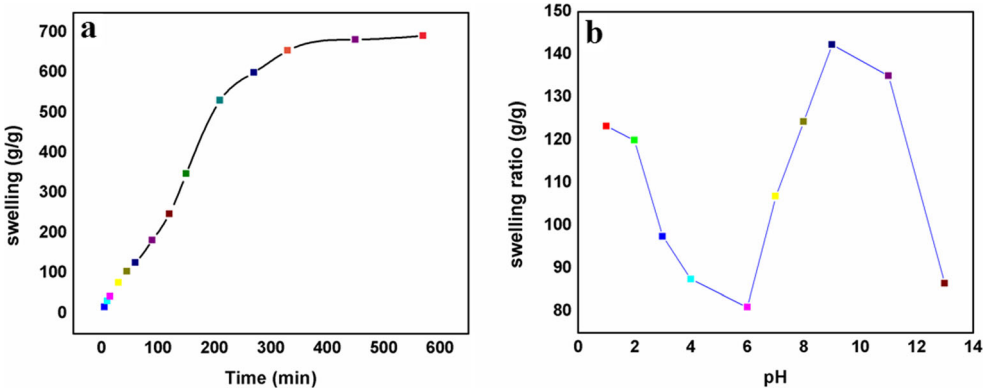

Fig. 5 Effect of contact (**a**) time and (**b**) pH on swelling behavior of BPCMC-g-poly (APTAC-co-DMA)

third degradation stage occurred at 567 °C which resulted in further loss in mass of 15 wt% leaving behind 9% residue which was taken as ash content of the prepared BPCMC-g-poly (APTAC-co-DMA) hydrogel. The observed difference in the stability/behavior of the prepared BPCMC-g-poly (APTAC-co-DMA) hydrogel and BPC extracted in response to heat is taken as supported evidence to affirm the grafting of APTAC and DMA onto BPCMC backbone [35].

Swelling studies (effect of pH and contact time)

Effect of pH and contact time

The swelling behavior of the prepared BPCMC-g-poly (APTAC-co-DMA) hydrogel was evaluated in order to determine the hydrogel's response to different pH environments. The pH sensitivity studies were prequel to the dye adsorption studies and were used as yardstick in selecting the optimum condition of pH and contact time to conduct dye uptake studies on the prepared hydrogel. Initially, the effect of contact time on the swelling capacity of the prepared hydrogel in distilled water was performed by soaking a known quantity of the prepared hydrogel in distilled water and the sample was taken at the preset time interval (0–570 min) until no further increase in water uptake was observed. This was used to ascertain the pH responsiveness of the prepared hydrogel. Solutions of varied pH (1–13) were prepared as per the procedure explained in sec. 2 and the study was run for a maximum contact time of 330 min (Fig. 5a). As illustrated in Fig. 5b, the prepared hydrogel exhibited maximum swelling capacity in pH 9 solution at a contact time of 330 min. it is observed that the swelling capacity of the prepared BPCMC-g-poly (APTAC-co-DMA) hydrogel decreases when the pH of the solution increases from pH (1–6) and increases from pH (7–10) before it later decreases with further increase in pH of the solution. The prepared BPCMC-g-poly (APTAC-co-DMA) hydrogel is proven to be pH sensitive and the maximum swelling was obtained in solution of pH 9. The variation in swelling capacity of the prepared hydrogel might be due to the fact that, the carboxylic group of the hydrogel ionizes differently when the pH of the swelling medium varies. The observed decrease in swelling capacity of the prepared hydrogel with increasing pH from 1 to 6 could be attributed to the ionic repulsion between the positively charged quaternary ammonium group and the abundant H^+ ion present at lower pH. This resulted in the expansion of the polymer network thereby leading to the penetration of enormous quantity of water into the polymer structure and by extension, a very high swelling. However, the high water uptake observed at high pH might be attributed to the ionization of some of the –COOH groups to $–COO^-$ ions leading to the increased water uptake ability of the prepared BPCMC-g-poly (APTAC-co-DMA) hydrogel [56].

Dye adsorption isotherms studies

Adsorption isotherms models are important tools that are used to delineate the nature of the interaction between the adsorbent and adsorbate at equilibrium. They are also used in the elucidation of the nature of the adsorbate distribution between the solid surfaces. The two most popular adsorption isotherms models which are used to illustrate the adsorption data are the Langmuir and Freundlich adsorption isotherm models. The linearized form of Langmuir adsorption isotherm model and Freundlich isotherm model are illustrated by Eqs. 6 and 7

Table 2 Isotherm models parameters for adsorption of Rh.B and E.B.T. onto BPCMC-g-poly (APTAC-co-DMA) hydrogel

Dye	Langmuir Isotherm			Freundlich Isotherm		
	q_e (mg/g)	k_L (L/mg)	R^2	n	k_F (L/mg)	R^2
Rhodamine B.	434.782	33.91	0.753	1.104	13.157	0.998
Eriochrome B.T.	714.285	101.428	0.751	1.136	8.281	0.997

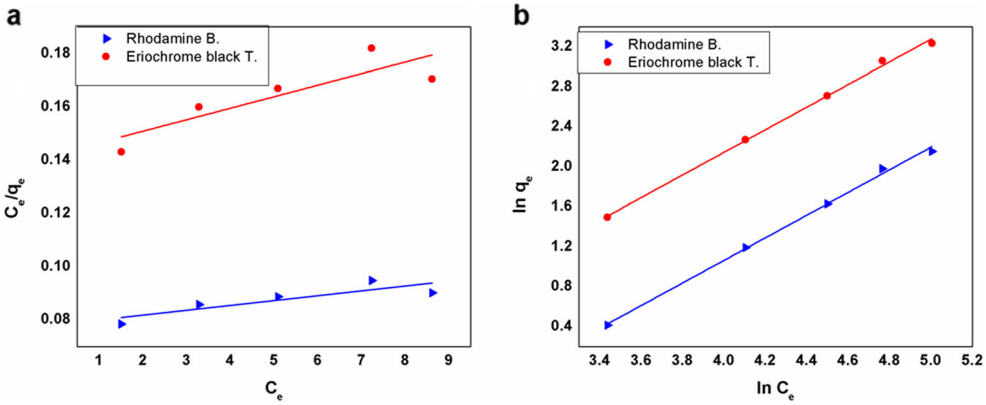

Fig. 6 Comparison of (**a**) Langmuir and (**b**) Freundlich isotherm models for RhB and Eriochrome black T. adsorption onto BPCMC-g-poly (APTAC-co-DMA) {pH =7, Dye concentrations = 50 mgL^{-1}, adsorbent dose = 49 mg100 mL^{-1}}

respectively.

$$\frac{C_e}{q_e} = \frac{1}{q_m} C_e + \frac{K_L}{q_m} \tag{6}$$

$$lnq_e = lnK_F + \frac{1}{n} lnC_e \tag{7}$$

Where C_e (mg/L) represents the dye concentration in solution at equilibrium, q_e (mg/g) stands for the amount of dye adsorbed at equilibrium, q_m (mg/g) represents the maximum adsorption capacity of the hydrogel, K_L and K_F (L/mg) represent the Langmuir and Freundlich constants and 1/n stands for the adsorption intensity. All corresponding parameters such as the Langmuir and Freundlich constants, adsorption intensity, equilibrium adsorption and correlation coefficient (R^2) were calculated from the slopes and intercept of linear plots of ln q_e against ln C_e and C_e/q_e against (Ce) for Freundlich and Langmuir adsorption isotherm models respectively and the result is as depicted in Table 2.

While Langmuir adsorption isotherm model illustrates the quantitative monolayer formation of the adsorbate on the adsorbent surface, the Freundlich adsorption isotherm presumes the multilayer adsorption of the adsorbate on the heterogeneous surface. There is non-uniform distribution of heat of adsorption on the heterogeneous surface. The favorability or otherwise of the adsorption process is determine from the value of the quantity (1/n) present in Freundlich isotherm model equation [57]. For 'n' value less than unity, the adsorption process is said to be favorable but when the value of 'n' exceeds unity, the adsorption process is said to be unfavorable. Usually, the adsorption process is said to follow certain isotherm model that is to say, Langmuir or Freundlich isotherm model if the value of correlation coefficient (R^2) approaches unity. As illustrated in Table 2, the adsorption of both Rhodamine B. and Eriochrome black T. cannot be elucidated by Langmuir adsorption isotherm model in the sense that, the value of correlation coefficient (R^2) is far from unity. Conversely, the adsorption of Rhodamine B. and Eriochrome black T. dyes onto BPCMC-g-poly (APTAC-co-DMA) can best be illustrated by Freundlich adsorption isotherm owing to the closeness of linear correlation coefficient (R^2) value to the unity. As illustrated in Table 2., the adsorption of Rhodamine B. and Eriochrome black T. dyes onto BPCMC-g-poly (APTAC-co-DMA) hydrogel is best explained by chemisorptions arising from strong ionic interaction between the dye molecules and the prepared hydrogel [57] (Fig. 6).

Effect of pH on adsorption

Because of the significant role it plays in the adsorption as it affect the surface binding sites of the prepared hydrogel and ionization process of dye molecules, studies on the effect of pH on dye adsorption were performed and the result is depicted in Fig. 7. Varied solution pH ranging from 1 to 13 for an initial dye concentration (100 mg/L for Rhodamine B and Eriochrome black T dyes were prepared and used for this study. The process lasted for 60 min with the adsorbent dosage of 50 mg. it can be deduced from Fig. 7 that the dye adsorption capacity of the prepared hydrogel increases with increase in the pH of the adsorption medium and was higher at pH 11

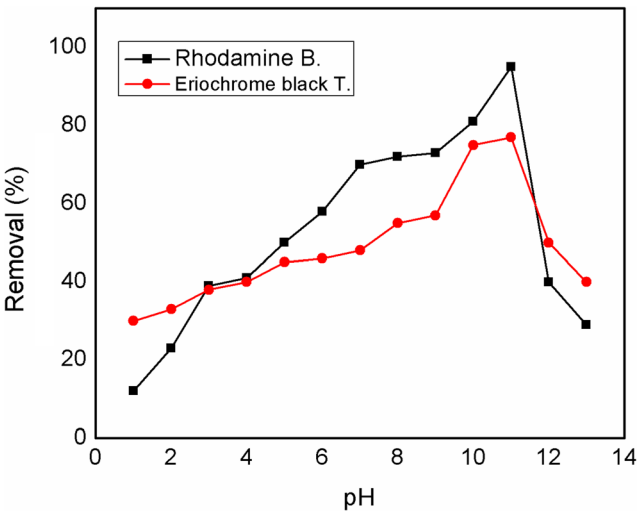

Fig. 7 Effect of pH on adsorption of Eriochrome black T and Rhodamine B. (initial dye concentration: 100 mg L^{-1})

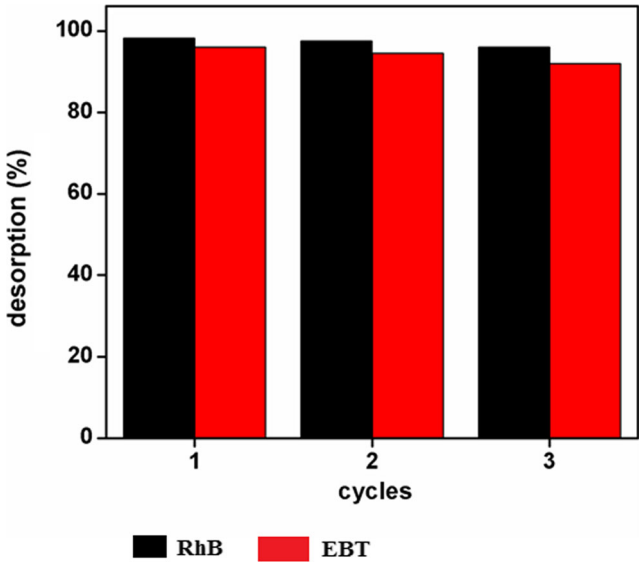

Fig. 8 Recycle of adsorbents for RhB and EBT adsorption (50 mg adsorbents; 50 mL; room temperature; 30 min)

with virtually 100% removals. This is due to the fact that in basic pH, dye adsorption occurs via strong interaction between –NMe3 of positively charged APTAC and negatively charged groups of the dye molecules. It is proposed therefore that the higher adsorption capacity of the prepared hydrogel at basic pH was effective in the diffusion of dye into the hydrogel matrix hence, an increase in the adsorption capacity.

Dye adsorption-desorption studies

Successive adsorption-desorption processes on the dyes used were performed in order to evaluate the reusability of the prepared hydrogel via three consecutive cycles. For the adsorption cycles, aqueous solutions of 50 mg L^{-1} of the dyes were stirred with the hydrogel at room temperature until the adsorption reaches equilibrium. The dye loaded hydrogel was subjected to the desorption process. Desorption process was carried out in acidic and basic conditions for cationic dye of Rhodamine B and anionic dye of Eriochrome black T respectively. The desorption experiment for Rhodamine B was performed in acidic medium, due to the protonation of negative COO − groups by H^+, which limits the electrostatic attraction between the surface of the adsorbent and the cationic dye of Rhodamine B which translate into an increase in its desorption ability from the adsorbent. As depicted in Fig. 8, Over 98.00% of Rhodamine B can be desorbed indicating the high performance of desorption capacity of the hydrogel. As for Eriochrome black T, the desorption experiment was performed under basic condition owing to the increasing number of deprotonated groups of COO− which would decrease the interaction between the surface of the adsorbent and the anionic dye of Eriochrome black T. The maximum percentage desorption for Eriochrome black T was found to be 96.00%. It was observed that the desorption process reached equilibrium within 30 min. The adsorption-desorption cycles result shown in Fig. 8, indicate that the percentage desorption was high for the three cycles with a very small decrease in the adsorption and desorption capacities over the course of several cycles. Thus, the hydrogel can repeatedly be utilized with negligible loss in adsorption capacity for the dyes used in this study.

Comparison of dye adsorption capacity of different adsorbents

The comparison between the adsorption capacities of the prepared BPCMC-g-poly (APTAC-co-DMA) hydrogel with other adsorbents reported in the literature is shown in Table 3. It is

Table 3 Comparison of maximum dye adsorption capacites of various hydrogels

Hydrogel	Dye	$q_{max}(mgg^{-1})$	Reference
BPCMC-g-poly (NaAc-co-AM)	Eriochrome black T.	714	This work
Coffee ground	Rhodamine B	187	[6]
Sokolymus hispanicus	Eriochrome B.T.	233	[7]
Rice Husk	Rhodamine B.	478	[54]
Peanut	Rhodamine B.	53.2	[58]
Pineapple peel/sepia ink hydrogel	Methylene blue	138.25	[47]
Cashew nut	Eriochrome B.T	160	[57]
Cashew nut shellPl-g-poly(APTAC)	Eriochrome B.T.	5.184	[59]
	Azocarmine B	113.6	[60]
Pl-polyacrylamide	Reactive blue	182	[61]
CMC-g-polyDAEMA	Methyl orange	182	[62]
CHT-g-PA Ac/RHA	Methylene blue	197	[63]
Poly (AA-co-NaAc-co-AM)	Azure-I	299.1	[17]
CNC/aliginate hydrogel beads	Methylene blue	256.41	[1]
CMC-g-poly(NaAc-co-AM)	Methylene blue	333.3	[48]

palpable that the prepared BPCMC-g-poly (APTAC-co-DMA) hydrogel exhibited extremely higher adsorption capacity (714 mg/g) towards dye in comparison to most of the adsorbents depicted in Table 3. This stipulates that the prepared BPCMC-g-poly (APTAC-co-DMA) hydrogel could thus be utilized as effective adsorbent for efficient removal of hazardous dye from industrial discharges.

Conclusion

An environmentally friendly superabsorbent hydrogel derived from banana pseudo-stem was synthesized via free radical graft copolymerization of (3-acrylamidopropyl)-trimethylammonium chloride and N,N-Dimethylacrylamide onto banana pseudo-stem carboxymethyl cellulose. Ammonium per sulfate and methylene bis acrylamide were used as initiator and cross linking agent respectively. The hydrogel was characterized for its structure, morphology and thermal property by FT-IR, FESEM and TGA analyses respectively. The pH sensitivity test conducted on the prepared BPCMC-g-poly (APTAC-co-DMA) hydrogel revealed its responsiveness towards change in pH of the tested solutions. Isotherm studies conducted on the prepared hydrogel revealed Freundlich isotherm models as befitting model describing the adsorption process. The prepared hydrogel exhibited extraordinarily higher water absorbance (559.37 g/g) and high dye sorption capacity of 714 and 434 mg/g for Eriochrome black T. and Rhodamine B. dyes respectively. This excellent water absorbency in comparison with the reported agric-waste-based hydrogels and pH responsiveness exhibited by the prepared hydrogel make it a suitable candidate not only in the area of modern agriculture, horticulture and waste water treatment, but also for use as a potential biomaterial for the slow release of fertilizers and controlled drug release.

References

1. Mohammed N, Grishkewich N, Berry RM, Tam KC (2015). Cellulose 22:3725
2. Ahuja S (2009) *Handbook of water purity and quality.* Elsevier, New York
3. Métivier-Pignon H, Faur-Brasquet C, Le Cloirec P (2003). Sep Purif Technol 31:3
4. Chequer FM, de Oliveira GA, Ferraz ER, Cardoso JC, Zanoni MV, de Oliveira DP (2013) InTech
5. Kono H, Ogasawara K, Kusumoto R, Oshima K, Hashimoto H, Shimizu Y (2016). Carbohydr Polym 152:170
6. Shen K, Gondal MA (2017) J Saudi Chem Soc, vol 21, p 120
7. Barka N, Abdennouri M, Makhfouk ME (2011). J Taiwan Inst Chem Eng 42:320
8. Kasperchik VP, Yaskevich AL, Bil'Dyukevich AV (2012) Wastewater treatment for removal of dyes by coagulation and membrane processes. Pet Chem 52:545–556
9. Mao J, Won SW, Min J, Yun YS (2008). Korean J Chem Eng 25: 1060
10. Gürses A, Yalçin M, Dogar C (2003). Water Air Soil Pollut 146:297
11. Hidalgo N, Mangiameli G, Manzano T, Zhadan GG, Kennedy JF, Shnyrov VL, Roig MG (2011). Biotechnol Bioprocess Eng 16:821
12. Rahmani AR, Godini K, Nematollahi D, Azarian G, Maleki S (2016). Korean J Chem Eng 33:532
13. Lin Q, Gao M, Chang J, Ma H (2016). Carbohydr Polym 151:283
14. Qiu M, Huang C (2015). Desalin Water Treat 53:3641
15. Zhang G, Yi L, Deng H, Sun P (2014). J Environ Sci 26:1203
16. Nadafi K, Vosoughi M, Asadi A, Borna MO, Shirmardi M (2014). J Water Chem Techno 36:125
17. Shukla NB, Madras G (2012). J Appl Polym Sci 124:3892
18. Pourjavadi A, Bassampour Z, Ghasemzadeh H, Nazari M, Zolghadr L, Hosseini SH (2016). J Polym Res 23:60
19. Nakhjiri MT, Bagheri Marandi G, Kurdtabar M (2018). J Polym Res 25:244
20. Mahdavinia GR, Massoumi B, Jalili K, Kiani G (2012). J Polym Res 19:9947
21. Ghasemzadeh H, Ghanaat F (2014). J Polym Res 21:1–14
22. Singha NR, Karmakar M, Mahapatra M, Mondal H, Dutta A, Roy C, Chattopadhyay PK (2017). Polym Chem 8:3211
23. Kajjari PB, Manjeshwar LS, Aminabhavi TM (2011). Ind Eng Chem Res 50:13280
24. Almomen A, Cho S, Yang CH, Li Z, Jarboe EA, Peterson CM, Huh KM, Janát-Amsbury MM (2015). Pharm Res 32:2266
25. Liu H, Zhang Y, Yao J (2014). Fiber Polym 15:145
26. Sato T, Uchida R, Tanigawa H, Uno K, Murakami A (2005). J Appl Polym Sci 98:731
27. Kaith BS, Jindal R, Kapur GS (2013). Iran Polym J 22:561
28. Lee E, Kim B (2011). Korean J Chem Eng 28:1347
29. Souda P, Sreejith L (2014). Polym Bull 71:839
30. Chen Z, Wang W, Guo L, Yu Y, Yuan Z (2013). SCIENCE CHINA Chem 56:1701
31. Bortolin A, Aouada FA, Mattoso LH, Ribeiro C (2013). J Agric Food Chem 61:7431
32. Li Q, Ma Z, Yue Q, Gao B, Li W, Xu X (2012). Bioresour Technol 118:204
33. Bashir S, Teo YY, Ramesh S, Ramesh (2018) K Polymer 31
34. Soleimani F, Sadeghi M, Shahsavari H (2012). Indian J Sci Technol 5:2041
35. Tally M, Atassi Y (2016). Polym Bull 73:3183
36. Mittal H, Kaith BS, Jindal R, Mishra SB, Mishra AK (2015). J Therm Anal Calorim 119:131
37. Ferfera-Harrar H, Aouaz N, Dairi N (2016). Polym Bull 73:815
38. Zhang M, Cheng Z, Zhao T, Liu M, Hu M, Li J (2014). J Agric Food Chem 62:8867
39. Zhou H, Zhu H, Yang X, Zhang Y, Zhang X, Cui K, Shao L, Yao J (2014). Bioresources 10:760
40. Bhattacharya D, Germinario LT, Winter WT (2008). Carbohydr Polym 73:371
41. Sun JX, Sun XF, Zhao H, Sun RC (2004). Polym Degrad Stab 84: 331
42. Li R, Wang S, Lu A, Zhang L (2015). Cellulose 22:339
43. Penjumras P, Rahman RB, Talib RA, Abdan K (2014). Agric Agric Sci Procedia 2:237
44. Huang R, Cao M, Guo H, Qi W, Su R, He Z (2014). J Agric Food Chem 62:4643
45. Musfiroh I, Hasanah AN, Budiman I (2013). RJPBCS 4:1092
46. Shanmugam N, Nagarkar RD, Kurhade M (2015) Indian J Nat Prod Resour 6:42

47. Khan MZ, Sarkar MA, Al Imam FI, Khan MZ, Malinen RO (2014). J Nat Fibers 11:199
48. Bello K, Sarojini BK, Narayana B, Rao A, Byrappa K (2018). Carbohydr Polym 181:605
49. Soleimani F, Sadeghi H, Shahsavari H, Soleimani A, Sadeghi F (2013). Asian J Chem 25:9
50. Hakam A, Rahman IA, Jamil MS, Othaman R, Amin MC, Lazim AM (2015). Sains Malaysiana 44:827
51. Istirokhatun T, Rokhati N, Rachmawaty R, Meriyani M, Priyanto S, Susanto H (2015). Procedia Environ Sci 23:274
52. Constantin M, Mihalcea I, Oanea I, Harabagiu V, Fundueanu G (2011). Carbohydr Polym 84:926
53. Haque MO, Mondal MI (2016). Raj Univ J Sci Eng 44:45
54. Nazir MS, Kassim MH, Mohapatra L, Gilani MA, Raza MR, Majeed K (2016). Polym Compos:35
55. Bhuyan MM, Okabe H, Hidaka Y, Hara K (2018). J Appl Polym Sci 135:45906
56. Dai H, Huang H (2017). J Agric Food Chem 65:565
57. d'Halluin M, Rull-Barrull J, Bretel G, Labrugère C, Le Grognec E, Felpin FX (2017). ACS Sustain Chem Eng 5:1965–1973
58. Mahdavinia GR, Asgari A (2013). Polym Bull 70:2451
59. Kumar PS, Ramalingam S, Senthamarai C, Niranjanaa M, Vijayalakshmi P, Sivanesan S (2010). Desalination 261:52
60. Constantin M, Asmarandei I, Harabagiu V, Ghimici L, Ascenzi P, Fundueanu G (2013). Carbohydr Polym 91(1):74–84
61. Samaneh S, Hayrettin OG, Saeed S, Mustafa G (2014). Water Air Soil Pollut:2177–2191
62. Salama A, Shukry N, El-Sakhawy M (2015). Int J Biol Macromol: 72–75
63. Marcelo GV, Antonio GBP, André RF, Antônio CNA & Francisco HAR (2017) Water Air Soil Pollut 228–241